Periodic Structure Containing Lossy Metamaterial and Defect Mode

Alireza Aghajamali[1], Tannaz Alamfard[1], and Arafa H. Aly[2,*]

[1]Department of Optics and Laser Engineering, Marvdasht Branch, Islamic Azad University, Marvdasht, Iran

[2]Department of Physics, Faculty of Sciences, Beni-Suef University, Egypt

Abstract: We theoretically investigate the properties of defect mode in one-dimensional lossy metamaterial photonic crystal doped with single-negative materials photonic-quantum-well (PQW). We examine the defect mode as a function of the type of negative index materials (NIMs) and the number of the unit cells of four different defected structures. The results obtained that the parameters; frequency, height, and the number defect modes can be tuned by varying the type of NIM in defect layers, PQW structure, and the unit cells as well in the defected structure. The defect modest end to show a shift in the frequency based on the particular type of NIM and the number of the unit cells. The results can lead to possible information for designing new types of narrow tunable filters at microwave frequency.

Keywords: Metamaterials, Defect mode, Photonic crystals, Negative index, Photonic-quantum-well.

1. INTRODUCTION

The concept of photonic crystals (PCs) was obtained first by Yablonovitch [1] and John [2]. They recognized that the propagation of electromagnetic waves could be controlled by using periodic modulation of dielectric media. The most fundamental optical property of a PC is the existence of photonic band gaps (PBGs), a particular frequency band in which the electromagnetic field is not able to propagate. In 1968, Veselago [3] predicted the negative-index material (NIM) with a permittivity and permeability simultaneously turns to a negative value. This material is also known as double-negative (DNG) material that is an artificial composite, contrary to the usual double-positive (DPS) material. According to the causality principle along with the Kramers-Kronig relations, NIMs are dispersive and lossy [4], and the presence of loss or dissipation influences the wave features [5-7]. According to an experimental viewpoint, DNG materials are obtained by making use of two types of single-negative (SNG) materials [8, 9]. In SNG materials either the material parameters or is negative. SNG materials with negative and positive are called epsilon-negative (ENG) materials, while materials with negative and positive are mu-negative (MNG) material. In recent years, metamaterial photonic crystals (MetaPCs) have been of great interest to the community for their particular properties. A wide range of research groups have focused on the unique features of PCs and MetaPCs scientific and engineering applications [10-23].

A defected crystal would be generated by breaking the periodicity of the conventional PC structure. This behavior can be performed by changing the thickness of one layer, inserting a defect layer into the structure, or removing a layer from the PC. In the defected structure, localized defect modes within the PBG would be generated owing to change the interference behavior of waves at interfaces. Such phenomenon resembles the existence of defect states in the forbidden band of doped semiconductors. A usual PC of $(CD)^M$ can insert into a host PC of $(AB)^N$ rather than a defect layer being added to the defected PC. Therefore, the structure will be $(AB)^{N/2}$ $(CD)^M$ $(AB)^{N/2}$, where N and M are the stack numbers of the (AB) and (CD) bilayers, respectively. In such case, the defected structure of $(CD)^M$ will be called the photonic-quantum-well (PQW) [24-26]. If one of the pass bands of PQW can be designed to overlap completely with one of the PBGs of the defected PC of $(AB)^N$. The structure $(AB)^{N/2}$ $(CD)^M$ $(AB)^{N/2}$ (with $M < N$) can present multiple filtering feature due to the photonic confinement, contributing to a perception of a multichannel filter [24]. Moreover, the number of channels that can consider as the basis of the number of peaks in the transmission spectra is equal to the stack number of PQW. Based on these observations, some multichannel narrowband transmission filters have so far been theoretically investigated in this regard [24-28], and some experimental studies applying the PQW have been conducted [29-30]. The multichannel filters help us to compose the dense wavelength division multiplexing filter in the different application. Despite the fact that there have been many reports on filters based on the basis of PQW [24-28], few studies examine tunable multichannel transmission filters.

*Address correspondence to this author at the Department of Physics, Faculty of Sciences, Beni-Suef University, Egypt;
Tel: +201220553834; Fax: +2082445555;
E-mail: arafaaly@aucegypt.edu; arafa.hussien@science.bsu.edu.eg

E-ISSN: 2408-977X/16

The main purpose of this paper is to conduct a theoretical investigation of the effects of the number of unit cells of PQW on the properties of defect modes for two different types of NIM defect layers. The 1D defected PC composed of DNG and DPS material layers with SNG materials PQW as a defect layer locate at the center of the structure. To achieve this goal, we will consider four different types of PQW defect. The first defected structure (Figure **1**(**a**)) containing a PQW defect is arranged as follow air/{(AB)$^{N/2}$ (ENG-DPS)^{M} (AB)$^{N/2}$}/air, where the PQW is (ENG-DPS)^{M}. The second one (Figure **1**(**a**)) with PQW as a defect layer assume as air/{(AB)$^{N/2}$ (MNG-DPS)^{M} (AB)$^{N/2}$}/air, where the PQW defect is (MNG-DPS)^{M}. The third structure (Figure **1**(**a**)) denoted as air/{(AB)$^{N/2}$ (MNG-ENG)^{M} (AB)$^{N/2}$}/air, and the last one is air/{(AB)$^{N/2}$ (MNG-DPS-ENG-DPS)^{M} (AB)$^{N/2}$}/air as shown in Figure **1**(**b**). The layers *A* and *B* are assumed to be DNG and DPS materials, respectively. *N* and *M* are the stack numbers of the (*AB*) and PQW structure, respectively. In the following calculations, we will apply the transmittance spectra to survey the properties of defect modes for both types of NIM defect layers in the last proposed four structures. The related transmittance spectra will achieve through the transfer matrix method (TMM) [31]. The outline of the paper arranged as follows. We introduce in section 2 the theoretical analysis of TMM and the description of permittivity and permeability of the two types of NIMs. Section 3 reveals the numerical results and discussions associated with our purpose, and Section 4 describes the conclusions of the investigation.

2. THEORETICAL FRAMEWORK

According to the TMM, the total transfer matrix for the whole system is obtained from the following equation [31],

$$M = \begin{pmatrix} m_{11} & m_{12} \\ m_{21} & m_{22} \end{pmatrix} = D_0^{-1}\left(\prod_{i=1}^{N} D_j P_j D_j^{-1}\right) P_s. \tag{1}$$

The above equation is considered for N-layers with a starting (input) medium 0 and a layer (output) behind the structure*S*. The propagating matrix *P* in layer *j* with a thickness L_j is written as

$$P_j = \begin{pmatrix} e^{ik_{jx}L_j} & 0 \\ 0 & e^{-ik_{jx}L_j} \end{pmatrix}. \tag{2}$$

Whenan electromagnetic wave propagates along the $+x$ direction in a medium, the corresponding wave number would be determined from equation $k_{jx} = \omega/c\, n_j \cos\theta_j$ where n_j, θ_j, ω and *c* are the refractive index, angle of incidence, the wave frequency, and the speed of wave in free space, respectively. According to Eq. (1), there is also a dynamical matrix for each layer in the multilayer system and can be expressed for the TE wave as follow,

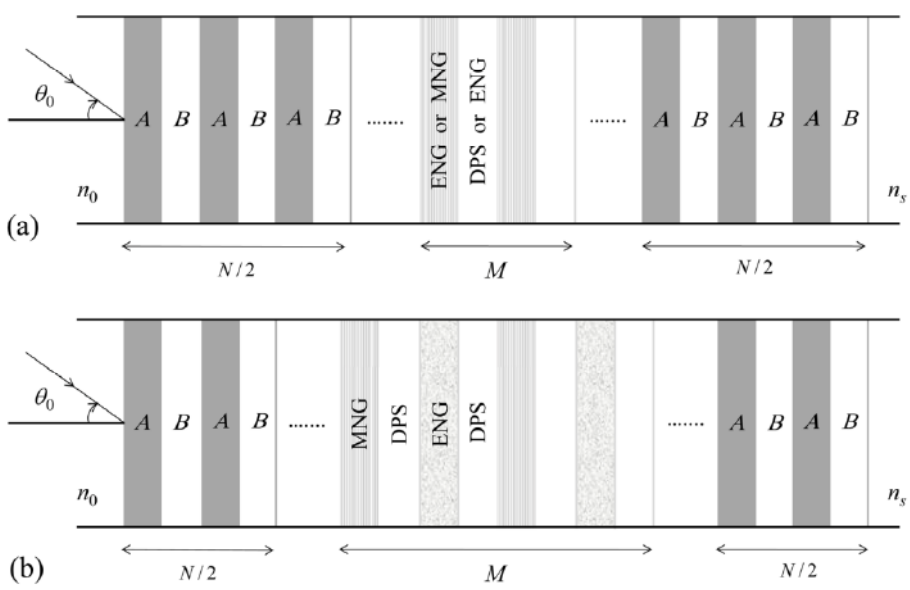

Figure 1: Schematic diagrams of 1D defected Meta PCs embedded in air, where layers *A* and *B* are DNG metamaterial and DPS material, respectively; (**a**) the first, second, and third structures with binary PQW defect, (**b**) the fourth PQW defected structure. *N* and *M* are respectively the numbers of the lattice period of the host PCs and PQW structure, and the incident angle is θ_0.

$$D_j = \begin{pmatrix} 1 & 1 \\ n_j \cos\theta_j & -n_j \cos\theta_j \end{pmatrix}, \quad (3)$$

and for the TM wave as follow,

$$D_j = \begin{pmatrix} \cos\theta_j & \cos\theta_j \\ n_j & -n_j \end{pmatrix}; \quad (4)$$

the transmission coefficient t for a multilayer system is given by $t = 1/m_{11}$,where m_{11} is an element of the total transfer matrix; consequently, the transmittance is calculated from relation,

$$T = \frac{n_s \cos\theta_s}{n_0 \cos\theta_0} t * t. \quad (5)$$

Our research is on the basis of two different types of NIMs. The following equations determine the complex permittivity and permeability of type-I NIM layer with negative refracting index in the microwave region [11, 32],

$$\varepsilon(f) = 1 + \frac{5^2}{0.9^2 - f^2 - i f \gamma_e} + \frac{10^2}{11.5^2 - f^2 - i f \gamma_e} \quad (6)$$

$$\mu(f) = 1 + \frac{3^2}{0.902^2 - f^2 - i f \gamma_m} \quad (7)$$

Various aspects of the real parts of the permittivity and permeability, ε' and μ', versus frequency have been discussed in more details and can be found in the previous reports [32-37]. In addition, the complex permittivity and the permeability will be determined within the framework of the Drude model for type-II NIM layer [38], namely

$$\varepsilon(f) = 1 - \frac{100}{f^2 - i f \gamma_e} \quad (8)$$

$$\mu(f) = 1.44 - \frac{100}{f^2 - i f \gamma_m}. \quad (9)$$

In the above-mentioned equations, f is the frequency given in GHz, and γ_e, γ_m are the electric and magnetic damping frequencies, respectively, (also it called the electric and magnetic loss factors) which are also measured in GHz. In Figure **2**, the change in ε' and μ' as a function of frequency is illustrated for both type-I and type-II NIMs (when $\gamma_e = \gamma_m = 2\times10^{-3}$ GHz). As observed from the figure, the real parts of both the permittivity and permeability of type-I NIM are simultaneously negative for $1.5 < f < 3.13$ GHz. Moreover, as shown in Figure **2**, in type-II NIM, both ε' and μ' are also negative for $1.5 < f < 3.13$ GHz. To conduct our investigations, we consider this range of frequencyin order to observe the zero-$\bar{n}$ gap [11, 32].

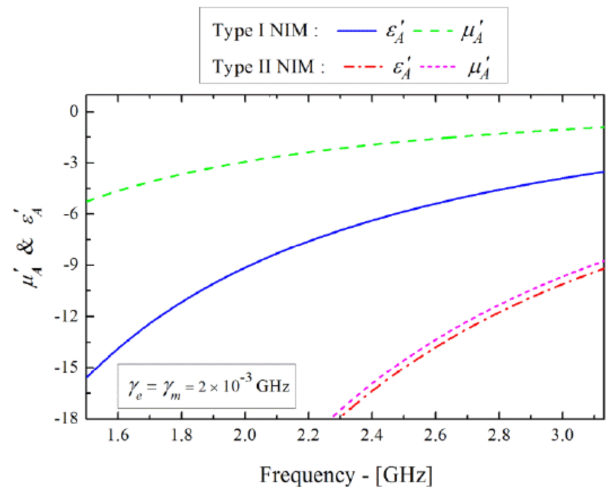

Figure2: Real parts of permittivity and permeability of two different types of NIMs, ε'_A and μ'_A, versus frequency when γ_e and γ_m are kept at $\gamma_e = \gamma_m = 2\times10^{-3}$ GHz.

3. NUMERICAL RESULTS AND DISCUSSION

The transmission spectrum of the lossy defected PC with an SNG met amaterial PQW defect at the center is calculated based on the theoretical model described in the previous section. Equations (6) and (7) are used for the permittivity and permeability of DNG layer (layer *A*). DPS layer (layer *B*) is assumed to be the vacuum layer with $n_B = 1$. In addition, for the PQW structure, the permittivity of ENG layer is considered as Eq. (6) for type-I NIM and Eq. (8) for type-II NIM while the permeability is taken as $\mu = 1$ (layer *C*). For layer *D;* MNG layer, Eqs. (7) and (9) are selected for the permeability of type-I and type-II NIMs and we assume that the permittivity is $\varepsilon = 1$. Moreover, the thicknesses of layers *A*, *B*, *C* and *D* are taken to be $d_A = 6$ mm and $d_B = d_C = d_D = 12$ mm, respectively. In addition, the total number of the lattice period is selected to be $N = 16$ [32]. We consider the case of normal incidence for the propagating waves in the four structures.

As mentioned before, we consider a 1D lossy defected MetaPC structure composed of four different types of PQW defect at the center of the host structure when it contains both type-I and type-II NIMs. Then, we will study the effects of the number of the unit cells of PQW (which corresponds to the central defect structure) on the defect modes that appear in the transmission spectra. In the first structure, Figure **1**(**a**), we consider the PQW defect as (ENG-DPS)^M. In Figure **3**, we can observe the changes in the defect mode features and transmission spectra as a function of frequency for various values of *M* for both type-I and type-II NIMs. We have clearly observed that, for the case of the structure contains type-I NIMs, a single defect mode appears in the photonic band gap. The height of such defect mode decreases and the defect mode is blue-shifted as *M* increases. In the case of type-II NIMs, a single defect mode emerges in the photonic band gap with increasing the value of *M*. Moreover, the associated defect mode behaves differently for odd and even values of *M*. However, the characteristics of the defect mode corresponding to odd numbers bear the resemblance to the even ones. For instance, when *M* is taken to be an odd number, as the value of *M* increases, the height of the appearing defect mode increases and starts to be red-shifted. Consequently, such behavior is also observed for even values of *M* while the position and feature of the appearing defect mode are completely different. In the other words, in the even case, the defect mode appears at a higher frequency compared with the odd one.

Also, for the second structure, Figure **1**(**a**), we consider our defected PQW as (MNG-DPS)^M. In Figure **4**, the transmission spectra as a function of frequency are plotted for various values of *M* for both type-I and type-II NIMs. In type-I NIM structure, with a rise in the value of *M*, there appears a single defect mode whose height decreases and shows a blue-shift. Furthermore, with an increase in the value of *M*, the rate of the total transmission slightly decreases. For the case of that structure contains type-II NIMs, a single defect mode is developed in the photonic band gap that behaves differently for odd and even values of *M*. As the value of *M* increases, the height of the defect mode increases for odd numbers of *M* while the height of the defect mode decreases for even numbers. Also, when *M* increases, a red-shift slightly occurs for both odd and even cases. Moreover, similar to the first structure, for the even values, the defect mode appears at a higher frequency close to the right band edge.

To be continued in this study, we consider the third defected structure has (MNG-ENG)^M as a PQW defect at the center of the host crystal, Figure **1**(**a**). Figure **5** demonstrates the changes in the defect modes and transmission spectra as a function of frequency for various values of *M* for both types of NIMs. As shown in the figure, when the structure contains type-I NIMs, the number of defect modes increases as *M* increases and the height of each defect mode slightly decreases. Moreover, each appearing defect mode is red-shifted

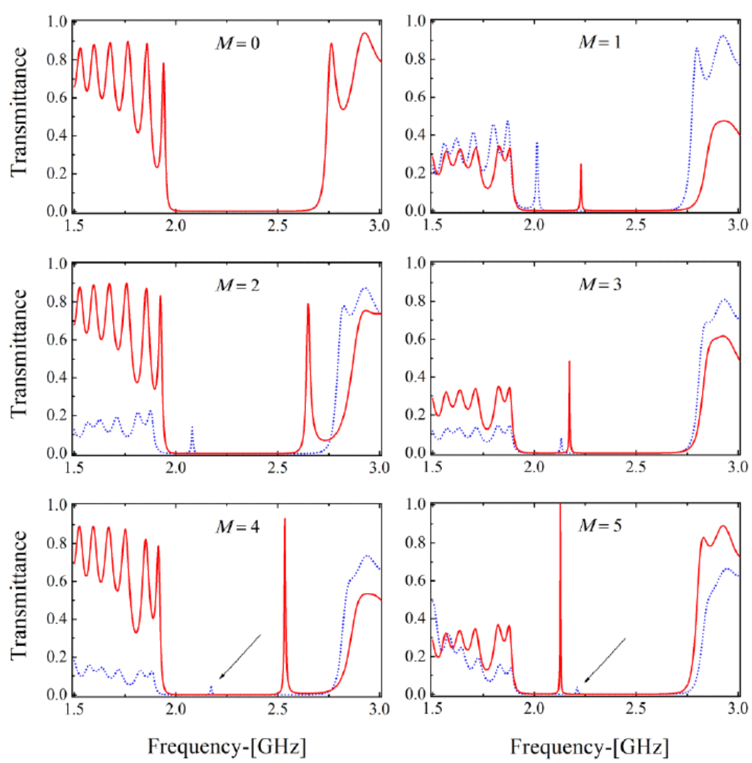

Figure 3: The transmission spectra as a function of incidence frequency for a 1D defective MetaPC structure when the PQW defect is (ENG-DPS)^M, for both type-I (blue dotted line) and type-II NIMs (red solid line) under various values of *M*.

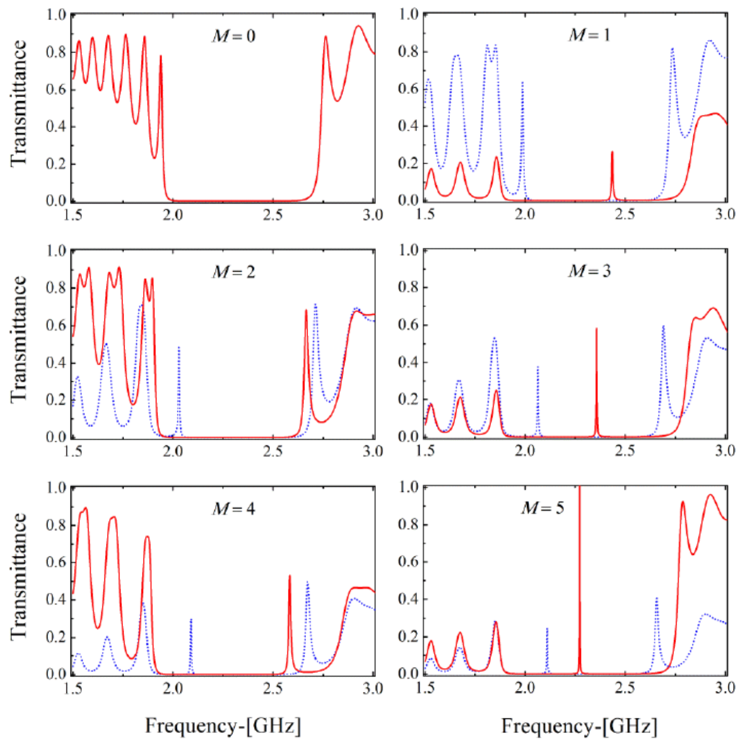

Figure 4: The transmission spectra as a function of incidence frequency for a 1D defective MetaPC structure when the PQW defect is $(\text{MNG-DPS})^M$, for both type-I (blue dotted line) and type-II NIMs (red solid line) under various values of *M*.

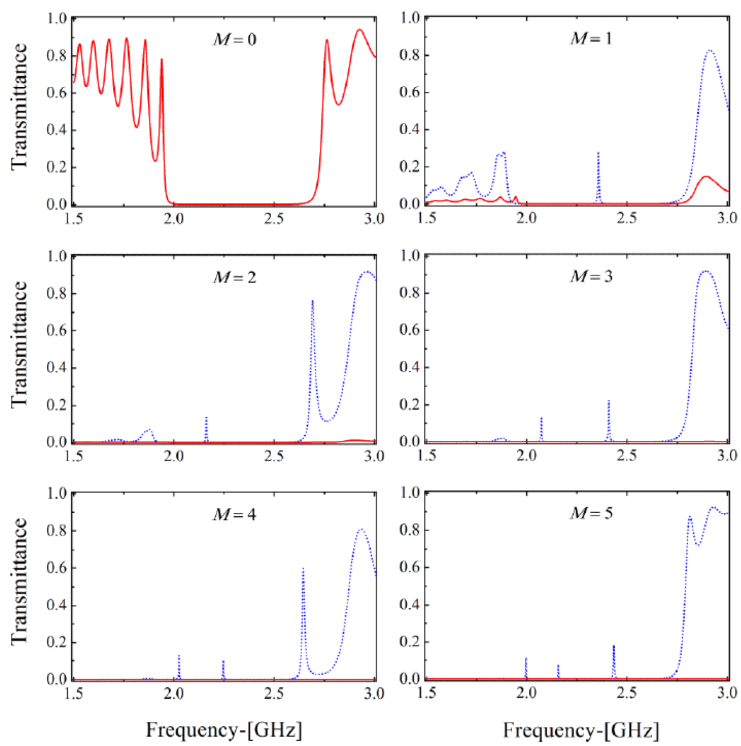

Figure 5: The transmission spectra as a function of incidence frequency for a 1D defective MetaPC structure when the PQW defect is $(\text{MNG-ENG})^M$, for both type-I (blue dotted line) and type-II NIMs (red solid line) under various values of *M*.

as a function of *M*. In the case of type-II NIMs, no defect modes exist in the photonic band gap and the rate of transmission spectra decreases sharply till the transmittance abruptly reaches zero as the value of *M* increases.

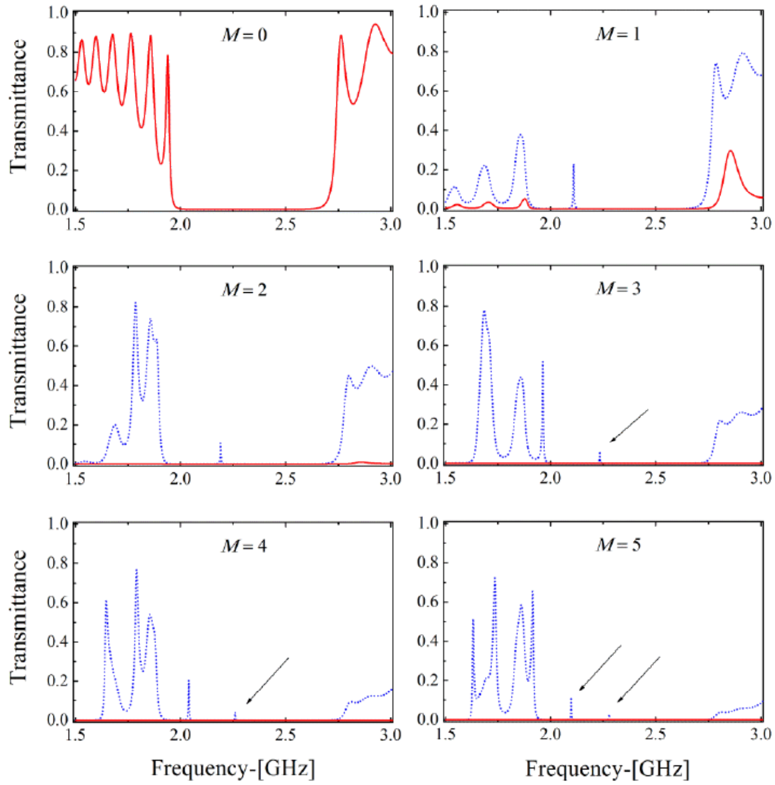

Figure 6. The transmission spectra as a function of incidence frequency for a 1D defective MetaPC structure when the PQW defect is (MNG-DPS-ENG-DPS)^M, for both type-I (blue dotted line) and type-II NIMs (red solid line) under various values of *M*.

The last defected structure, Figure **1**(**b**), contains (MNG-DPS-ENG-DPS)^M as a PQW defect at the center of the host crystal. In Figure **6**, we examine the role played by various values of *M* in the transmission spectra as a function of frequency for both types of NIMs. We can see that, if the structure composed of type-I NIMs, a single defect mode developed within the photonic band gap by increasing *M*. The height of the related single defect mode decreases and appears to be blue-shifted as *M* increases. In addition, it is noteworthy that as the associated defect mode disappears, a new defect mode with similar behaviors and characteristics will be developed. For the case of type-II NIMs, analogous to the previous results mentioned in Figure **5**, no defect modes appeared in the photonic band gap and the rate of transmission spectra dramatically decreases till it suddenly reaches zero value. This behavior is mainly because the fact that the difference in the dispersion relations in ε and μ for these two types of NIM. The type-I is a Lorentz form whereas it is a Drude type for the type-II.

Based on the results mentioned above, we find that the defect mode of such MetaPCs contain PQW defect is very sensitive to the types of NIMs and the number of the PQW unit cell. Also, it is strongly dependent on the considered defected structure. Based on these detailed analyses, we can present constructive information that can contribute to design new types of narrowband and multichannel transmission filters.

4. CONCLUSION

In this paper, we have theoretically studied the properties of four different 1D defective MetaPCs structure containing PQW defect. The numerical results of our study illustrate the variation of the PQW defect layer, the type of the NIMs, and the number of the unit cells of PQW structure can strongly change the properties and the number of the defect modes. For instance, these associated efficient factors could determine whether the defect modes should appear or disappear. Also, they have great effect son the defect modes height and position through the frequency range. In the first and second structures, in the case of type-I NIM, by increasing *M*, the height of the defect mode decreases and shows a blue-shift. However, type-II NIM case shows opposite trends, and the defect mode behaves differently for odd and even values of *M*. For the third and fourth structures, in the case of type-I NIM, the height and number of the defect mode increases and shifts to a higher frequency; on the other hand, in the type-II NIM case, the transmission spectra, and following that, the defect modes dramatically decrease till the transmittance seems to fall toward zero. The output information and results obtained from the properties of the produced defect modes arising from such defective PC with PQW defect would be beneficial in designing new types of tunable narrow microwave filter which are able to be applied in optical communications.

REFERENCES

[1] Yablonovitch E. "Inhibited spontaneous emission in solid-state physics and electronics," Phys Rev Lett 1987; 58: 2059. https://doi.org/10.1103/PhysRevLett.58.2059

[2] John S. "Strong localization of photons in certain disordered dielectric superlattices," Phys Rev Lett 1987; 58: 2486. https://doi.org/10.1103/PhysRevLett.58.2486

[3] Veselago VG. "The electrodynamics of substances with simultaneously negative values of and, " Sov Phys Usp 1968; 10: 509. https://doi.org/10.1070/PU1968v010n04ABEH003699

[4] N. Engheta, RW. Ziolkowski, Metamaterials: Physics and Engineering Explorations (John Wiley & Sons, Singapore, 2006). https://doi.org/10.1002/0471784192

[5] Sabah C. Uckun S. "Electromagnetic wave propagation through frequency-dispersive and lossy double-negative slab," Opto-Electron. Rev 2007; 15: 133 . https://doi.org/10.2478/s11772-007-0011-y

[6] Canto JR, Matos SA, Paiva CR, Barbosa AM. "Effects of losses in layered structure containing DPS and DNG media," PIERS Online, 2008; 4: 546. https://doi.org/10.2529/PIERS071220142320

[7] Hsu HT, Ting KC, Yang TJ, Wu CJ. "Investigation of photonic band gap in a one-dimensional lossy DNG/DPS photonic crystal," Solid State Commun 2010; 150: 644. https://doi.org/10.1016/j.ssc.2009.12.027

[8] Smith DR, Padilla WJ, Vier DC, Nemat-Nasser SC, Schultz S. "Composite Medium with Simultaneously Negative Permeability and Permittivity," Phys. Rev. Lett 2000; 84: 4184. https://doi.org/10.1103/PhysRevLett.84.4184

[9] Shelby RA, Smith DR, Schultz S. "Experimental Verification of a Negative Index of Refraction," Science 2001; 292: 77. https://doi.org/10.1126/science.1058847

[10] Gerardin J, Lakhtakia A. "Negative index of refraction and distributed Bragg reflectors," Microwave Opt. Technol. Lett 2002; 34: 409. https://doi.org/10.1002/mop.10478

[11] Li J, Zhou L, Chan CT and Sheng P. "Photonic band gap from a stack of positive and negative index materials," Phys. Rev. Lett 2003; 90: 083901. https://doi.org/10.1103/PhysRevLett.90.083901

[12] Jiang H, Chen H, Li H, Zhang Y, Zi J, Zhu S. "Properties of one-dimensional photonic crystals containing single-negative materials," Phys. Rev. E 2004; 69: 066607. https://doi.org/10.1103/PhysRevE.69.066607

[13] Shadrivov I, Sukhorukov A, Kivshar Y "Complete Band Gaps in One-Dimensional Left-Handed Periodic Structures," Phys. Rev. Lett 2005; 95: 193903. https://doi.org/10.1103/PhysRevLett.95.193903

[14] Elsayed HA, El-Naggar SA, Aly AH. "Thermal properties and two-dimensional photonic band gaps," J. Modern Opt 2014; 61: 385. https://doi.org/10.1080/09500340.2014.887155

[15] Essa MF and Arafa H Aly, " CR-39 track detector as a photonic crystal" J. Comput. Theor. Nanosci 2013; 6:1527-1531. https://doi.org/10.1166/jctn.2013.2884

[16] Elsayed HA, El-Naggar SA, Aly AH. "Two dimensional tunable photonic crystals and n doped semiconductor materials," Mater. Chem. Phys 2015; 160: 221. https://doi.org/10.1016/j.matchemphys.2015.04.027

[17] Aly AH, El-Naggar SA, Elsayed HA. "Tunability of two dimensional n-doped semiconductor photonic crystals based on the Faraday effect," Opt. Express 2015; 23: 15038. https://doi.org/10.1364/OE.23.015038

[18] Arafa H Aly, Elsayed HA and H Hamdy "The optical transmission characteristics in metallic photonic crystals" Materials Chemistry and Physics 2010; 124: 856-860. https://doi.org/10.1016/j.matchemphys.2010.08.006

[19] Arafa H Aly, Hanafey HS " Polarization modes control on the transmittance characteristics of one dimensional photonic crystal" J. Comput. Theor. Nanosci 2011; 8: 1916-1919. https://doi.org/10.1166/jctn.2011.1901

[20] Arafa H. Aly, Hussein A. Elsayed and Sahar El-Naggar A. " Tuning the flow of light in two-dimensional metallic photonic crystals based on Faraday effect" J modern optics 2017; 64: 1, 74-80. https://doi.org/10.1080/09500340.2016.1208298

[21] [21 Arafa H Aly " Superconductor-Dielectric Photonic Band Gap in Ultraviolet Radiation" International Journal of Advanced Applied Physics Research, Special Issue 2016; 43-47: 43, E-ISSN: 2408-977X/16.

[22] Arafa H Aly and wailed Sayed, " Superconductor-Semiconductor metamaterial photonic crystals" J Supercond Nov Magn 2016; 29: 1981-1986. https://doi.org/10.1007/s10948-016-3478-2

[23] Arafa H Aly, Alireza Aghajamali, Hussein Elsayed A and Mohamed Mobarak" Analysis of cutoff frequency in a one-dimensional superconductor-metamaterial photonic crystal, Physica C 2016; 528: 5-8. https://doi.org/10.1016/j.physc.2016.05.025

[24] Qiao F, Zhang C, Wan J, Zi J. "Photonic quantum-well structures: Multiple channeled filtering phenomena," Appl. Phys. Lett 2000; 77: 3698. https://doi.org/10.1063/1.1330570

[25] Chen X, Lu W, Shenv SC. "Photonic resonant transmission in the quantum-well structure of photonic crystals," Solid State Commun 2003; 127: 541. https://doi.org/10.1016/S0038-1098(03)00509-X

[26] Bian T, Zhang Y. "Transmission properties of photonic quantum well composed of dispersive materials," Optik 2009; 120: 736. https://doi.org/10.1016/j.ijleo.2008.03.003

[27] Feng CS, Mei LM, Cai LZ, Li P, Yang XL. "Resonant modes in quantum well structure of photonic crystals with different lattice constants," Solid State Commun; 2005; 135: 330. https://doi.org/10.1016/j.ssc.2005.04.040

[28] Xu C, Xu X, Han D, Liu X, Liu CP, Wu CJ. "Photonic quantum-well structures containing negative-index materials," Optics Commun 2007; 280: 221. https://doi.org/10.1016/j.optcom.2007.07.041

[29] Xu SH, Xiong ZH, Gu LL, Liu Y, Ding XM, Zi J, Hou XY. "Photon confinement in one-dimensional photonic quantum-well structures of nanoporous silicon," Solid State Commun 2003; 126: 125. https://doi.org/10.1016/S0038-1098(02)00892-X

[30] Yano S, Segawa Y, Bae JS. "Quantized state in a single quantum well structure of photonic crystals," Phys Rev B 2001; 63: 153316. https://doi.org/10.1103/PhysRevB.63.153316

[31] Yeh P. Optical Waves in Layered Media (John Wiley & Sons Inc., NY, 2005).

[32] Aghajamali A and Barati M. "Effects of normal and oblique incidence on zero- gap in periodic lossy multilayer containing double-negative materials," Phys. B: Condensed Matter 2012; 407: 1287. https://doi.org/10.1016/j.physb.2012.01.125

[33] Aghajamali A, Alamfard T and Barati M. "Effects of loss factors on zero permeability and zero permittivity gaps in 1D photonic crystal containing DNG materials," Phys. B: Condensed Matter 2014; 454: 170 . https://doi.org/10.1016/j.physb.2014.07.067

[34] Aghajamali A, Akbarimoosavi AM and Barati M. "Properties of the band gaps in 1D ternary lossy photonic crystal containing double-negative materials," Adv. Opt. Technol. 1, Article ID 129568 (2014). https://doi.org/10.1155/2014/129568

[35] Aghajamali A and Barati M. "Properties of defect modes in periodic lossy multilayer with negative index materials, " Commun. Theor Phys 2013; 60: 80. https://doi.org/10.1088/0253-6102/60/1/11

[36] Aghajamali A, Hayati M, Wu CJ and Barati M. "Properties of the defect modes in 1D lossy photonic crystals containing two types of negative-index-materials defects," J. Electromagn. Waves Appl 2013; 27: 2317. https://doi.org/10.1080/09205071.2013.843475

[37] Aghajamali A, Javanmardi B, Barati M and Wu CJ. "Defect modes properties in periodic lossy multilayer containing negative index materials with symmetric and asymmetric geometries structures," Optik 2014; 125: 839. https://doi.org/10.1016/j.ijleo.2013.07.016

[38] Chen Y. "Broadband one-dimensional photonic crystal wave plate containing single-negative materials," Opt. Express 2010; 18: 19920. https://doi.org/10.1364/OE.18.019920

Received on 14-11-2016 Accepted on 20-12-2016 Published on 28-12-2016

http://dx.doi.org/10.15379/2408-977X.2016.03.02.01